ISSN (Print) 1226-1750
ISSN (Online) 2233-6656
Journal of Magnetics 23(4), 639-643 (2018) https://doi.org/10.4283/JMAG.2018.23.4.639

Voltage-Control Spintronics Memory (VoCSM) with Low Write Current using Highly-Selective Patterning Process

M. Shimizu*, Y. Ohsawa, H. Yoda, S. Shirotori, B. Altansargai, N. Shimomura, Y. Kato, S. Oikawa, H. Sugiyama, T. Inokuchi, K. Koi, M. Ishikawa, K. Ikegami, and A. Kurobe

Toshiba Corporation, 1, Komukai-Toshiba-cho, Saiwai-ku, Kawasaki 212-8582, Japan

(Received 17 July 2018, Received in final form 22 October 2018, Accepted 6 November 2018)

A voltage-control spintronics memory (VoCSM) which has a potential of low energy consumption uses the spin-Hall effect (SHE) and the voltage-controlled magnetic anisotropy (VCMA) effect for its write operation. In this work, the relationship between the critical switching current (Ic_{sw}) and the SHE electrode thickness (t_N) is investigated in the range of 5 nm < t_N < 8 nm. In the fabrication process, we develop highly-selective patterning process to stop MTJ etching precisely on the surface of the SHE electrode. Using the technique, Ic_{sw} is reduced by half as t_N is varied from 8 nm to 5 nm, and Ic_{sw} of 112 mA at 20 ns write current pulse is obtained for MTJ size of 50 × 150 nm^2 on Ta(2 nm)/TaB (3 nm) electrode. The results indicate that the decrease in the SHE electrode thickness is a promised method to reduce Ic_{sw}, which leads VoCSM to a low-energy-consumption device.

Keywords : MRAM, critical switching current, spin-Hall effect, spin-orbit torque, VoCSM

1. Introduction

Magnetic random access memories (MRAMs) have been attracting much attention as nonvolatile memories having potentials of low energy consumption and high-speed writing. A voltage-control spintronics memory (VoCSM) is a novel nonvolatile memory, which has at least one magnetic tunnel junction (MTJ) with a storage layer/a tunneling barrier/a reference layer on a non-magnetic electrode in which a spin current is generated by spin-Hall effect (SHE) [1, 2]. The write operation of VoCSM has the following feature. SHE spin torque drives the magnetization switching of the storage layer. The critical switching current (Ic_{sw}) of the storage layer with in-plane anisotropy is modulated by applying control voltage to the MTJ element due to a voltage-controlled magnetic anisotropy (VCMA) effect [3].

Ic_{sw} by SHE spin torque is theoretically reduced linearly to the SHE electrode width and the SHE electrode thickness, respectively [4]. So there are the following two approaches to reduce Ic_{sw}. One is the decrease in the SHE electrode width. As for the SHE electrode width dependence of Ic_{sw}, we recently reported the experimental result for a self-aligned VoCSM structure which showed the reduction in Ic_{sw} linearly proportional to MTJ size as was theoretically expected [5]. The other is the decrease in the SHE electrode thickness. As for the SHE electrode thickness dependence of Ic_{sw}, it is important to develop a new fabrication process for VoCSM with thinner SHE electrode, as the electrode has to be 2 or 3 nm over-milled and causes the rise in the resistance of the SHE electrode using the conventional fabrication process.

In this study, we propose a highly-selective patterning fabrication process to stop the etching of MTJ film precisely on the surface of the electrode. Using the highly-selective patterning process, a self-aligned VoCSM structure with a thin SHE electrode was fabricated so as to reduce Ic_{sw}.

2. Experimental Procedure

MTJ elements with in-plane anisotropy were fabricated by masks and photolithography techniques on a SHE electrode on a thermal oxidized Si wafer. The SHE electrode of Ta (2 nm or 5 nm)/TaB (3 nm) was sputter-deposited on the wafer. Then the MTJ stack which has a

*Corresponding author: e-mail: mariko8.shimizu@toshiba.co.jp

This paper was presented at the IcAUMS2018, Jeju, Korea, June 3-7, 2018.

storage layer of $Fe_{80}B_{20}$ (2.2 nm), MgO tunneling barrier layer and a reference layer of CoFeB (1.8 nm)/Ru (0.9 nm)/CoFe (1.8 nm)/IrMn (8 nm) was sputter-deposited. The resistance-area product (*RA*) of MTJ element was around 1 kΩμm^2. These stacks were annealed at 300 degree C for 1 hour to pin the magnetization of CoFe. As for the detail of the SHE electrode, Ta layer was a seed layer for TaB layer, so the thickness of Ta layer was reduced so as to reduce Ic_{sw}. TaB layer had a larger spin-Hall angle (θ_{SH}) than Ta layer. θ_{SH} was estimated to be 0.18 in the TaB electrode and 0.09 in the Ta electrode by spin-Hall magnetoresistance (SMR) measurement method [6].

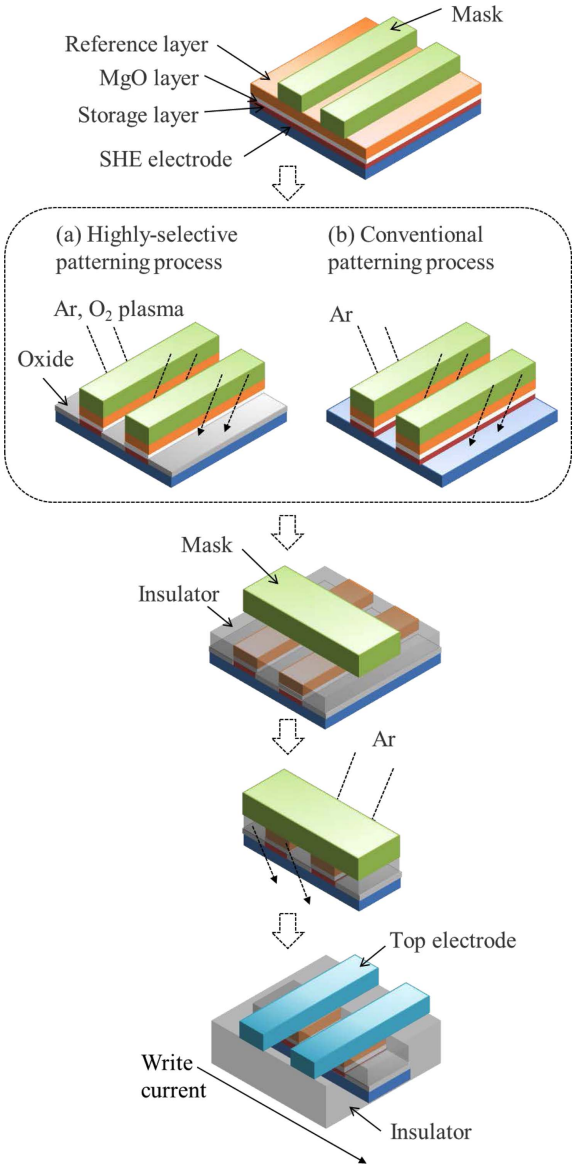

Fig. 1. (Color online) The schematic illustration of the fabrication process for a self-aligned VoCSM structure using a highly-selective patterning process (a) and using a conventional patterning process (b).

The schematic illustration of the fabrication process for a self-aligned VoCSM structure is shown in Fig. 1. Masks were fabricated across the write-current-flowing direction. Then, MTJ film was patterned using two types of fabrication processes: In a conventional patterning process as indicated in (b), MTJ film was ion-milled to the surface of the SHE electrode using the masks. In a highly-selective patterning process as indicated in (a), MTJ film was ion-milled to MgO barrier layer using the masks, and the film besides the storage layers was deactivated in O_2 plasmas to the surface of the SHE electrode using the same masks. After these patterning processes, second masks were fabricated along the write-current-flowing direction. Then the stack and the SHE electrode were ion-milled using the same masks. Finally, top electrodes were fabricated. MTJ size was around 50 nm × 150 nm and the width of SHE electrode was around 150 nm.

As shown in the cross-sectional transmission electron microscopy (TEM) images of VoCSM structures, the finished thickness of the SHE electrode was uniform using highly-selective patterning process in Fig. 2(a), while the electrode was 2.5 nm over-milled using a conventional patterning process in Fig. 2(b). Moreover, no oxidation damage was observed in the storage layer by O_2 plasmas in highly-selective patterning process from the TEM image and the electron energy-loss spectroscopy

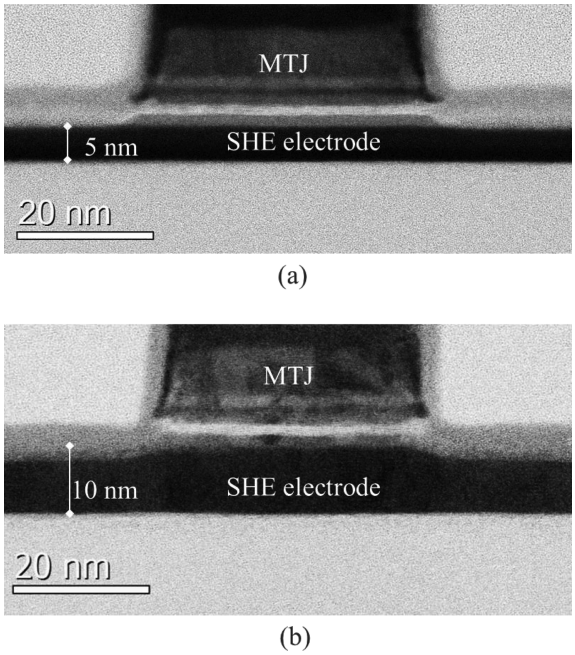

Fig. 2. The cross-sectional TEM images for a self-aligned VoCSM structure fabricated using a highly-selective patterning process (a) and using a conventional patterning process (b).

(EELS).

3. Results and Discussion

Figure 3 shows the resistance of an MTJ element as a function of write current with the control voltage of 1.2 V (a) and −1.2 V (b). The pulse widths of the write current pulse and the control voltage pulse were 20 ns. The critical switching current (Ic_{sw}) of 95 μA was obtained with the control voltage of −1.2 V and Ic_{sw} of 121 μA was obtained with the control voltage of +1.2 V. It was demonstrated that Ic_{sw} was modulated by applying the control voltage to the MTJ element due to VCMA effect.

The SHE electrode thickness (t_N) was decreased from 8 nm of Ta (5 nm)/TaB (3 nm) to 5 nm of Ta (2 nm)/TaB (3 nm) in order to reduce Ic_{sw}. Fig. 4(a) shows Ic_{sw} at 20 ns write current pulse without the control voltage as a function of MTJ size (w_{FS}·w_{FL}). Here, w_{FS} and w_{FL} are designed sizes of the storage layer along the SHE electrode and across the electrode, respectively, as indicated in Fig. 4(b). Ic_{sw} of the storage layer was 223 μA on Ta (5 nm)/TaB (3 nm) electrode and 112 μA on Ta (2 nm)/TaB (3 nm) electrode. The critical switching current density

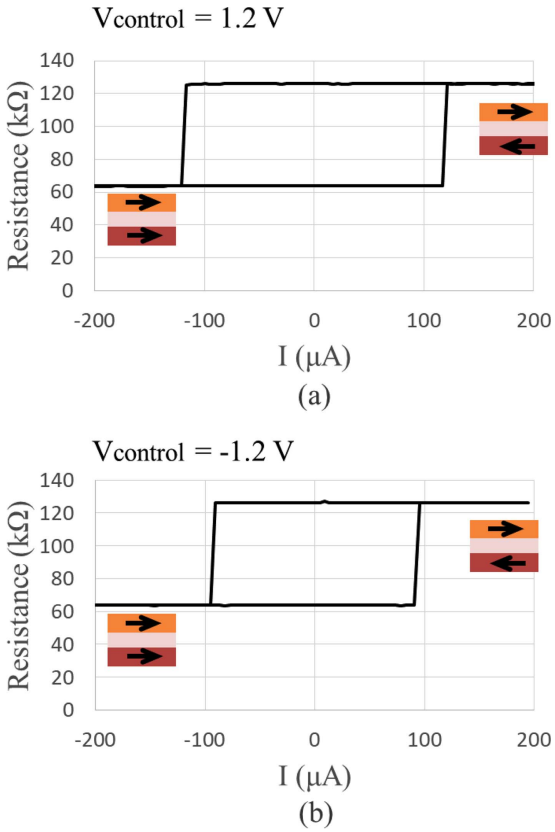

Fig. 3. (Color online) MTJ resistances as a function of write current with the control voltage of 1.2 V (a) and −1.2 V (b). The pulse widths were 20 ns.

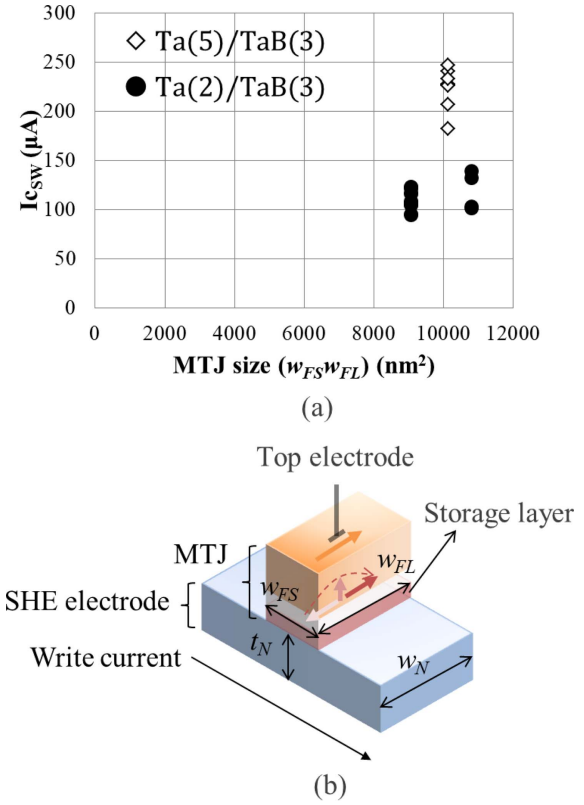

Fig. 4. (Color online) The critical switching current (Ic_{sw}) at 20 ns write current pulse without the control voltage as a function of MTJ size (w_{FS}·w_{FL}) for a self-aligned VoCSM structure with the SHE electrode of Ta (2 nm or 5 nm)/TaB (3 nm) (a) and the schematic illustration of the fabricated device (b).

(Jc_{sw}) of the storage layer was calculated to be 15.4 MA/cm^2 on Ta (5 nm)/TaB (3 nm) electrode and 12.0 MA/cm^2 on Ta (2 nm)/TaB (3 nm) electrode using the Ta/TaB bilayer thickness under the MTJ element.

Figure 5 shows Ic_{sw} at 20 ns write current pulse without the control voltage as a function of the SHE electrode thickness (t_N). The experimental results are analyzed by the following equation. Ic_{sw} is given by the equation (1):

$$I_{c_{sw}} = \frac{4e}{\hbar}\frac{\alpha}{\theta_{SH}}\Delta E_{sw}\frac{w_N t_N}{w_{FS} w_{FL}} \tag{1}$$

with

$$\Delta E_{sw} = V_{MTJ}\frac{M_s}{2}\left(H_c - \frac{H_{k-perp}}{2}\right) \tag{2}$$

$$V_{MTJ} \equiv w_{FS} w_{FL} t_f \tag{3}$$

Here, e, α, $\hbar$, ΔE_{sw}, w_N, t_N, V_{MTJ}, t_f, H_c and $H_{k\text{-}perp}$ are electron charge, the damping constant of the storage layer, reduced Planck's constant, the switching energy barrier of the storage layer, SHE electrode width, SHE electrode

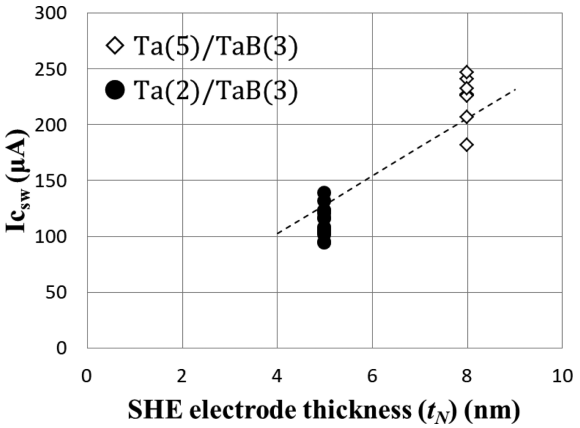

Fig. 5. Ic_{sw} at 20 ns write current pulse without the control voltage as a function of the SHE electrode thickness (t_N) with w_N of 185 nm. The dashed line is the result of a least-square fit by equation (1).

thickness, the storage layer volume, the storage layer thickness, the coercive field of the storage layer and the effective perpendicular magnetic anisotropy field of the storage layer. We carry out a least-square fitting by equation (1) and estimate θ_{SH} to be 0.10 under the assumption that ΔE_{sw} is 517 k_BT and α is 0.008. Here, ΔE_{sw} is calculated from the designed values H_c = 792 Oe, H_k = −3250 Oe and M_s = 1076 emu/cc using equation (2). In this analysis, the reduction in Ic_{sw} is assumed to be proportional to the electrode thickness. The dashed line in Fig. 5 indicates that the decrease in t_N is a promised method to reduce Ic_{sw}.

It is necessary to consider the relationship between Jc_{sw} and t_N in order to investigate a write efficiency. By taking account of the spin diffusion length in the SHE electrode, Jc_{sw} in the electrode of a thickness t_N is expected to be reduced from the bulk value by the equation (5) [7]:

$$J_{c_{sw}}(t_N) = I_{c_{sw}} \big/ w_N t_N \tag{4}$$

$$J_{c_{sw}}(t_N) \big/ J_{c_{sw}}(\infty) = 1 - \mathrm{sech}(t_N / \lambda_s) \tag{5}$$

where λ_s is a spin diffusion length of the electrode. When t_N is decreased to be a dimension comparable to λ_s, there seems to be a possibility of a reduction in Jc_{sw} by equation (5). The reported value of λ_s in the TaB electrode was 1.06 nm by spin-Hall magnetoresistance (SMR) measurement method [6]. λ_s may have much effect on Jc_{sw} when t_N is less than 5 nm. In the future, the highly-selective patterning process can be applied to fabricate a self-aligned VoCSM structure with ultra-thin SHE electrode due to its uniformity of the finished thickness of the electrode.

The resistivity (ρ) was 157 μΩcm for Ta electrode and 216 μΩcm for TaB electrode. The SHE electrode resistance per bit is much smaller than the MTJ element resistance. The resistance is calculated to be 0.3 kΩ for 5 nm thick SHE electrode per bit and around 100 kΩ for MTJ element, using the electrode width of 40 nm, the electrode length per bit of 40 nm, the resistance-area product (RA) of MTJ element of 100 Ωμm^2 and MTJ size of 20 nm × 40 nm.

4. Conclusion

In order to reduce Ic_{sw}, we have developed a highly-selective patterning fabrication process to stop MTJ etching precisely on the surface of the SHE electrode. The finished thickness of the electrode was uniform by using the pattering process. Moreover, no damage by the process was observed in the storage layer. Then, the relationship between Ic_{sw} and t_N was investigated for a self-aligned VoCSM structure with Ta (2 nm)/TaB (3 nm) electrode and Ta (5 nm)/TaB (3 nm) electrode. Ic_{sw} was reduced by half as t_N is varied from 8 nm to 5 nm, and Ic_{sw} of 112 μA was obtained at 20 ns write current pulse without the control voltage for the MTJ size around 50 × 150 nm^2. It was concluded that the fabrication of thinner SHE electrode is a promised method to reduce Ic_{sw}, which leads the self-aligned VoCSM structure to a low-energy-consumption device.

Acknowledgements

This work was partly supported by the ImPACT Program of the Council for Science, Technology and Innovation (Cabinet Office, Government of Japan).

References

[1] H. Yoda, N. Shimomura, Y. Ohsawa, S. Shirotori, Y. Kato, T. Inokuchi, Y. Kamiguchi, B. Altansargai, Y. Saito, K. Koi, H. Sugiyama, S. Oikawa, M. Shimizu, M. Ishikawa, K. Ikegami, and A. Kurobe, IEDM Tech. Dig. (2016) pp 2761-2764.

[2] T. Inokuchi, H. Yoda, Y. Kato, M. Shimizu, S. Shirotori, N. Shimomura, K. Koi, Y. Kamiguchi, H. Sugiyama, S. Oikawa, K. Ikegami, M. Ishikawa, B. Altansargai, A. Tiwari, Y. Ohsawa, Y. Saito, and A. Kurobe, Appl. Phys. Lett. **110**, 252404 (2017).

[3] T. Maruyama, Y. Shiota, T. Nozaki, K. Ohta, N. Toda, M. Mizuguchi, A. A. Tulapurkar, T. Shinjo, M. Shiraishi, S. Mizukami, Y. Ando, and Y. Suzuki, Nature Nanotechnology **4**, 158 (2009).

[4] Luqiao Liu, Chi-Feng Pai, Y. Li, H. W. Tseng, D. C. Ralph, and R. A. Buhrman, Science **336**, 555 (2012).

[5] S. Shirotori, H. Yoda, Y. Ohsawa, N. Shimomura, T. Inokuchi, Y. Kato, Y. Kamiguchi, K. Koi, K. Ikegami, H.

Sugiyama, M. Shimizu, B. Altansargai, S Oikawa, M. Ishikawa, A. Tiwari, Y. Saito, and A. Kurobe, IEEE. Trans. Magn. **53**, 3401104 (2017).
[6] Y. Kato, Y. Saito, H. Yoda, T. Inokuchi, S. Shirotori, N. Shimomura, S. Oikawa, A. Tiwari, M. Ishikawa, M. Shimizu, B. Altansargai, H. Sugiyama, K. Koi, Y. Ohsawa, and A. Kurobe, Phys. Rev. Applied, **10**, 044011 (2018).
[7] Luqiao Liu, Takahiro Moriyama, D. C. Ralph, and R. A. Buhrman, Phys. Rev. Lett. **106**, 036601 (2011).